PROCEEDINGS OF THE ROYAL SOCIETY A MATHEMATICAL, PHYSICAL & ENGINEERING SCIENCES

Diffraction by a plane sector

Bair V. Budaev and David B. Bogy

Proc. R. Soc. Lond. A 2004 **460**, 3529-3546
doi: 10.1098/rspa.2004.1322

10.1098/rspa.2004.1322

THE ROYAL SOCIETY

Diffraction by a plane sector

By Bair V. Budaev and David B. Bogy

Department of Mechanical Engineering, University of California, Berkeley, CA 94720, USA
(budaev@me.berkeley.edu; dbogy@me.berkeley.edu)

Received 15 January 2003; revised 29 January 2004; accepted 19 March 2004; published online 9 September 2004

The problem of diffraction by a perfectly reflecting screen occupying an infinite sector of the equatorial plane is addressed by the random-walk method. The solution is represented as a superposition of the wave field completely determined by an elementary ray analysis and of the field formed by the waves diffracted by the tip of the screen. The diffracted field is explicitly represented as the mathematical expectation of a specified functional on trajectories of the random motion, the radial component of which runs in a complex space while the two-dimensional angular component remains real valued. The numerical results confirm the efficiency of the random-walk approach to the analysis of diffraction by wedge-shaped screens of arbitrary angles.

Keywords: wave propagation; diffraction; ray method; Brownian motion

1. Introduction

It was recently shown (Budaev & Bogy 2003*a*) that problems of wave propagation in conical domains can be addressed by a combination of the Liouville product representation of wave fields, which is a common tool of ray theory, and the random-walk method, which delivers exact Feynman–Kac solutions (Dynkin 1965; Freidlin 1985) of second-order differential equations. This combination approach starts in a way that is similar to the ray method, in the sense that the solution of the Helmholtz equation $\nabla^2 U + k^2 U = 0$ is represented in the Liouville form $U = \mathrm{e}^{\mathrm{i}kr} u$, where r is a spherical radius. Then, instead of following the ray method, where the amplitude $u(r, \theta, \phi)$ is determined from the approximate first-order transport equation $\nabla r \cdot \nabla u + (\nabla^2 r)u = 0$, this amplitude is determined from the complete transport equation $(1/2\mathrm{i}k)\nabla^2 u + \nabla r \cdot \nabla u + (\nabla^2 r)u = 0$, whose exact solution is provided by the Feynman–Kac formula.

The fundamentals of the random-walk approach to wave propagation were outlined in Budaev & Bogy (2001, 2002*a*,*b*), where it was also shown that, in certain circumstances, the exact solutions of the Helmholtz equation provided by the random-walk method degenerate to the well-known asymptotes of the ray method. In Budaev & Bogy (2002*a*), it was shown that the random-walk method, as an exact approach, makes it possible to describe such typical phenomena of wave propagation as backscattering, which is predicted neither by the ray theory nor by a more general method of parabolic equations (Fock 1965; Fock & Leontovich 1946). In Budaev & Bogy (2003*a*), the method was applied specifically to problems in two-dimensional

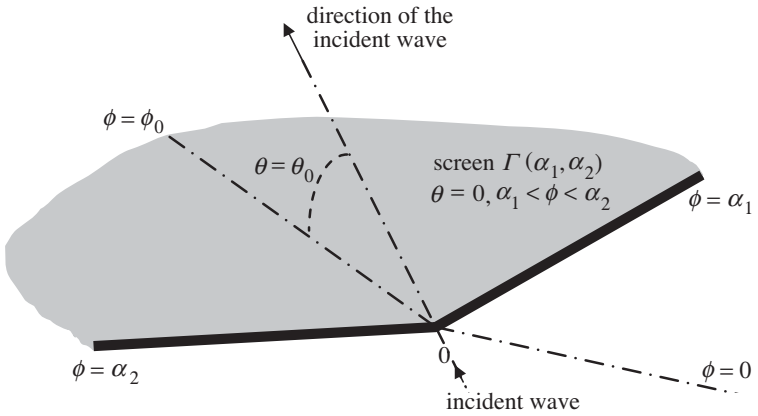

Figure 1. Configuration of the problem.

wedge-shaped domains and to three-dimensional problems in conical domains. These results were used in Budaev & Bogy (2004*c*) for the analysis of two-dimensional problems of wave scattering by surface breaking cavities and cracks of virtually arbitrary shape. In Budaev & Bogy (2003*b*), the method was adapted to problems of wave propagation in exterior cylindrical and spherical domains.

Here we continue our development of the random-walk approach to wave propagation and apply it to the important problem of diffraction by a wedge-shaped screen occupying a sector of the equatorial plane. Using the method from Budaev & Bogy (2003*a*), we obtain explicit formulae for the solution and illustrate their usefulness by computations for screens of several different angles.

2. Formulation of the problem and the structure of its solution

Let (r, θ, ϕ) be spherical coordinates in the three-dimensional space $\mathbb{R}^3$ defined as

$$r \geqslant 0, \quad -\tfrac{1}{2}\pi \leqslant \theta \leqslant \tfrac{1}{2}\pi, \quad 0 \leqslant \phi < 2\pi, \tag{2.1}$$

and let $\boldsymbol{e} = (1, \theta, \phi)$ denote the unit vector originating from the centre of the coordinates and ending at the point $x = (1, \theta, \phi)$. Then the field

$$U_0 \equiv U_0(r, \theta, \phi; \theta_0, \phi_0) = \mathrm{e}^{\mathrm{i}kr[\sin\theta \sin\theta_0 + \cos\theta \cos\theta_0 \cos(\phi - \phi_0)]} \tag{2.2}$$

describes a plane wave propagating along the direction $\boldsymbol{e}_0 = (1, \theta_0, \phi_0)$.

We are interested in the problem of diffraction of the incident wave U_0 by a reflecting sector

$$\Gamma \equiv \Gamma(\alpha_1, \alpha_2) : r > 0, \quad \theta = 0, \quad 0 < \alpha_1 < \phi < \alpha_2 < 2\pi, \tag{2.3}$$

positioned in the equatorial plane of $\mathbb{R}^3$, as illustrated in figure 1.

More precisely, the goal is to compute the solution of the Dirichlet problem

$$\nabla^2 U + k^2 U = 0, \qquad U|_\Gamma = 0, \tag{2.4}$$

which is defined in the conical domain

$$G = \mathbb{R}^3 \setminus \Gamma \tag{2.5}$$

and obeys the radiation condition at infinity, requiring that U not contain any waves arriving from infinity, except for the incident wave U_0 in (2.2).

It should be noted that the sole reason for limiting this paper to the problem with the Dirichlet boundary condition $U|_\Gamma = 0$ is to simplify the presentation of the novel method by restricting it to the basic case where only the principal ideas of the probabilistic approach to the differential equations of wave propagation are employed. The exploration of further capabilities of the method will be the subject of a separate paper employing a slightly more general, but still well-known, probabilistic technique that makes it possible to solve a broad class of problems with the boundary conditions (Budaev & Bogy 2004*a*,*b*)

$$gl\left[U + \mu_\pm \frac{\partial U}{\partial \boldsymbol{n}} gr\right]_{\Gamma_\pm} = 0, \tag{2.6}$$

containing different impedances $\mu_\pm$ on the different sides $\Gamma_\pm$ of the angular screen $\Gamma(\alpha_1, \alpha_2)$.

Elementary ray theory suggests (Felsen & Marcuvitz 1972) that the total wave field U can be decomposed into the sum,

$$U = U_\mathrm{s} + U_\mathrm{r} + U_1 + U_2 + \sum_{m=1}^{M} (U_1^m + U_2^m) + U_\mathrm{d}, \tag{2.7}$$

of several piecewise continuous wave fields, each of which has a distinctive physical meaning. Thus U_s represents the 'plane' wave coinciding with the incident wave outside the shadow zone $\mathfrak{G}_\mathrm{s}$, which is formed by the rays that are parallel to the incident direction $\boldsymbol{e}_0 = (1, \theta_0, \phi_0)$ and originating from the screen $\Gamma(\alpha_1, \alpha_2)$. Similarly, U_r represents the plane reflected wave propagating in the domain $\mathfrak{G}_\mathrm{r}$ symmetric to $\mathfrak{G}_\mathrm{s}$ with respect to the equator $\theta = 0$. The fields U_1 and U_2 are formed by cylindrical or, more precisely, by conical waves diffracted by the corresponding edge $\phi = \alpha_1$ or $\phi = \alpha_2$ of the screen. These waves propagate inside the cones $\mathfrak{G}_n$, $n = 1, 2$, obtained by the revolution of the ray $(\theta, \phi) = (\theta_0, \phi_0)$ around the edges $(\theta, \phi) = (0, \alpha_n)$ of $\Gamma(\alpha_1, \alpha_2)$. The conical waves U_n may generate a finite number of secondary conical waves U_1^m and U_2^m with $m = 1, 2, \ldots, M$, formed by the following process: if the cone $\mathfrak{G}_1$ contains the edge $\phi = \alpha_2$, then the field U_1 interacts with this edge and generates another conical wave U_1^1; similarly, if $\mathfrak{G}_2$ contains the edge $\phi = \alpha_1$, then U_2 generates a secondary conical wave U_2^1; in the next step, the waves U_1^1 and U_2^1 may also reach the other edges. An elementary analysis shows that there can be only a finite number of secondary conical waves and that all of them may be explicitly described by exact analytical formulae based on the well-known solution of the two-dimensional Sommerfeld problem of diffraction. Finally, U_d is the field formed by the waves diffracted by the tip of the screen, and this is the only component of (2.7) that is, until now, unknown.

To describe in more detail the individual terms of the decomposition (2.7), we introduce two sets of cylindrical coordinates $(\varrho_n, \vartheta_n, \zeta_n)$ associated with the edges of the screen $\Gamma(\alpha_1, \alpha_2)$ in such a way that the axis ζ_n coincides with the edge $\phi = \alpha_n$, and the polar angle $\vartheta_n \in [0, 2\pi)$ has the value $\vartheta_n = 0$ on the upper side of Γ. An elementary geometrical analysis shows that such coordinates $(\varrho_n, \vartheta_n, \zeta_n)$ are related

to the spherical coordinates (r,θ,ϕ) by the formulae

$$\varrho_n = r\sqrt{1-\cos^2\theta\cos^2(\phi-\alpha_n)}, \tag{2.8}$$

$$\tan\vartheta_n = \frac{\tan\theta}{\sin(\phi-\alpha_n)}, \tag{2.9}$$

$$\zeta_n = r\cos\theta\cos(\phi-\alpha_n), \tag{2.10}$$

with the values of ϑ_n fixed by the conditions

$$\vartheta_n \in \begin{cases} [0,\pi] & \text{if } \theta \geqslant 0, \\ [\pi,2\pi] & \text{if } \theta \leqslant 0. \end{cases} \tag{2.11}$$

Expressed in the coordinates $(\varrho_n,\vartheta_n,\zeta_n)$, the incident wave U_0 from (2.2) has the form

$$U_0 = \mathrm{e}^{\mathrm{i}k[\zeta_n\zeta_n^0+\varrho_n\varrho_n^0\cos(\vartheta_n-\vartheta_n^0)]}, \tag{2.12}$$

where $(\varrho_n^0,\vartheta_n^0,\zeta_n^0)$ are the cylindrical coordinates of the direction $\boldsymbol{e}_0=(1,\theta_0,\phi_0)$ of the incident wave. From equation (2.12), it easily follows that the shadow domain $\mathfrak{G}_{\mathrm{s}}=\mathfrak{G}_{\mathrm{s}}^1\cup\mathfrak{G}_{\mathrm{s}}^2$ consists of two cones

$$\left.\begin{aligned} \mathfrak{G}_{\mathrm{s}}^1 &= \{r>0,\ \alpha_1<\phi<\phi_0,\ 0<\vartheta_1<\vartheta_1^0\}, \\ \mathfrak{G}_{\mathrm{s}}^2 &= \{r>0,\ \phi_0<\phi<\alpha_2,\ 0<\vartheta_2<\vartheta_2^0\}, \end{aligned}\right\} \tag{2.13}$$

which are described in spherical coordinates (r,θ,ϕ) by

$$\left.\begin{aligned} \mathfrak{G}_{\mathrm{s}}^1 &: 0<\tan\theta\sin(\phi_0-\alpha_1)<\tan\theta_0\sin(\phi-\alpha_1), \quad \alpha_1<\phi\leqslant\phi_0, \\ \mathfrak{G}_{\mathrm{s}}^2 &: 0<\tan\theta\sin(\alpha_2-\phi_0)<\tan\theta_0\sin(\alpha_2-\phi), \quad \phi_0\leqslant\phi<\alpha_2. \end{aligned}\right\} \tag{2.14}$$

Similarly, the cones $\mathfrak{G}_{\mathrm{r}}^1$ and $\mathfrak{G}_{\mathrm{r}}^2$, illuminated by the reflected waves, are described by the inequalities

$$\left.\begin{aligned} \mathfrak{G}_{\mathrm{r}}^1 &: 0>\tan\theta\sin(\phi_0-\alpha_1)>-\tan\theta_0\sin(\phi-\alpha_1), \quad \alpha_1<\phi\leqslant\phi_0, \\ \mathfrak{G}_{\mathrm{r}}^2 &: 0>\tan\theta\sin(\alpha_2-\phi_0)>-\tan\theta_0\sin(\alpha_2-\phi), \quad \phi_0\leqslant\phi<\alpha_2. \end{aligned}\right\} \tag{2.15}$$

As for the straight and reflected fields U_{s} and U_{r} in (2.7), they are defined by the obvious formulae

$$U_{\mathrm{s}}(r,\theta,\phi) = \begin{cases} 0 & \text{inside } \mathfrak{G}_{\mathrm{s}}=\mathfrak{G}_{\mathrm{s}}^1\cup\mathfrak{G}_{\mathrm{s}}^2, \\ U_0(r,\theta,\phi;\theta_0,\phi_0) & \text{outside } \mathfrak{G}_{\mathrm{s}}=\mathfrak{G}_{\mathrm{s}}^1\cup\mathfrak{G}_{\mathrm{s}}^2, \end{cases} \tag{2.16}$$

and

$$U_{\mathrm{r}}(r,\theta,\phi) = \begin{cases} -U_0(r,\theta,\phi;-\theta_0,\phi_0) & \text{inside } \mathfrak{G}_{\mathrm{r}}=\mathfrak{G}_{\mathrm{r}}^1\cup\mathfrak{G}_{\mathrm{r}}^2, \\ 0 & \text{outside } \mathfrak{G}_{\mathrm{r}}=\mathfrak{G}_{\mathrm{r}}^1\cup\mathfrak{G}_{\mathrm{r}}^2, \end{cases} \tag{2.17}$$

where U_0 is the incident wave from (2.2).

Figure 2 shows projections of the cones $\mathfrak{G}_{\mathrm{s}}^1$, $\mathfrak{G}_{\mathrm{s}}^2$ and $\mathfrak{G}_{\mathrm{r}}^1$, $\mathfrak{G}_{\mathrm{r}}^2$ onto the (ϕ,θ)-plane. The presented example corresponds to the case when the sector $\Gamma(0^\circ,100^\circ)$ is illuminated by the incident wave propagating in the direction $\boldsymbol{e}_0=(1,50^\circ,30^\circ)$. The

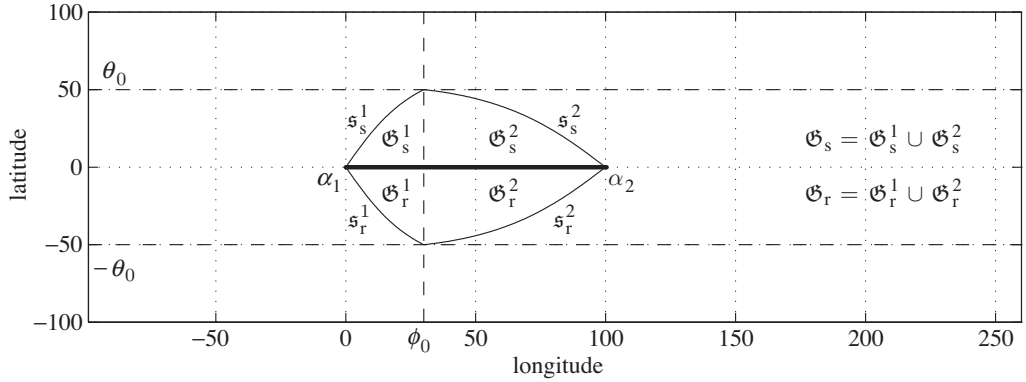

Figure 2. Domains $\mathfrak{G}_a$ and $\mathfrak{G}_r$ on the angular plane (ϕ, θ).

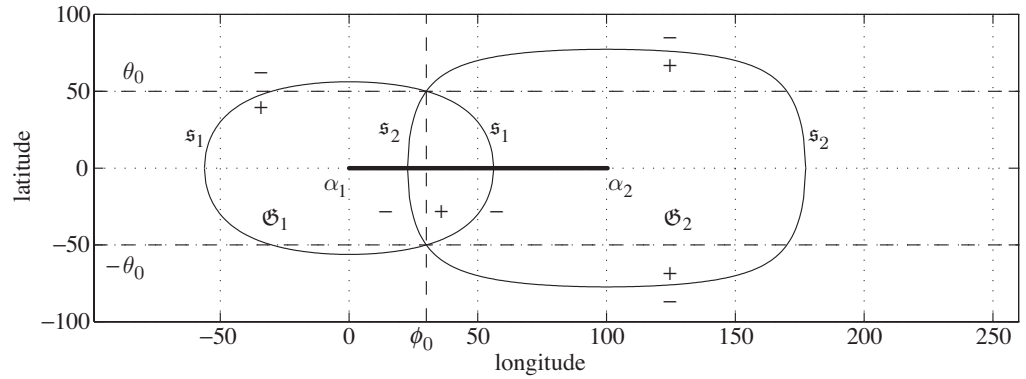

Figure 3. Conic domains $\mathfrak{G}_1$ and $\mathfrak{G}_2$ in spherical coordinates (ϕ, θ).

screen is located on the equatorial segment $\theta = 0$, $0° < \phi < 100°$, shown by the bold line. The cones $\mathfrak{G}_s^1$ and $\mathfrak{G}_s^2$ are located in the northern hemisphere $\theta > 0$ between the screen and the surfaces $\mathfrak{s}_s^1$ and $\mathfrak{s}_s^2$, which have a common ray $(\theta, \phi) = (\theta_0, \phi_0)$. Similarly, the cones $\mathfrak{G}_r^1$ and $\mathfrak{G}_r^2$ are located in the southern hemisphere between the screen and the surfaces $\mathfrak{s}_r^1$, $\mathfrak{s}_r^2$, which are symmetric to $\mathfrak{s}_s^1$, $\mathfrak{s}_s^2$, respectively.

Next we describe the domains $\mathfrak{G}_1$ and $\mathfrak{G}_2$ illuminated by the waves diffracted by the edges $(\theta, \phi) = (0, \alpha_1)$ and $(\theta, \phi) = (0, \alpha_2)$ of the screen $\Gamma(\alpha_1, \alpha_2)$. From ray theory, it follows that these waves propagate inside the cones described in the cylindrical coordinates $(\varrho_n, \vartheta_n, \zeta_n)$ as

$$\mathfrak{G}_n : \varrho_n \varrho_n^0 < \zeta_n \zeta_n^0, \quad 0 \leqslant \vartheta_n < 2\pi, \quad n = 1, 2, \tag{2.18}$$

where ϱ_n^0 and ζ_n^0 are the cylindrical coordinates of the direction $\boldsymbol{e}_0 = (1, \theta_0, \phi_0)$ of propagation of the incident wave. Then, applying the conversion formulae (2.10), (2.11), we find that, in the spherical coordinates (r, θ, ϕ), these cones are specified by

$$\mathfrak{G}_n : \begin{cases} \cos\theta \cos(\phi - \alpha_n) > \cos\theta_0 \cos(\phi_0 - \alpha_n) & \text{if } \cos(\phi_0 - \alpha_n) > 0, \\ \cos\theta \cos(\phi - \alpha_n) < \cos\theta_0 \cos(\phi_0 - \alpha_n) & \text{if } \cos(\phi_0 - \alpha_n) < 0. \end{cases} \tag{2.19}$$

Samples of the cones $\mathfrak{G}_1$ and $\mathfrak{G}_2$ projected onto the (θ,ϕ)-plane are shown in figure 3, which corresponds to the case of the screen $\Gamma(0^\circ,100^\circ)$ illuminated by the incident wave propagating along the vector $\boldsymbol{e}_0=(1,50^\circ,30^\circ)$. The cone $\mathfrak{G}_1$ is bounded by the smooth surface $\mathfrak{s}_1$ surrounding the left edge $\phi=\alpha_1=0^\circ$ of the screen, and $\mathfrak{G}_2$ is bounded by the surface $\mathfrak{s}_2$ surrounding the other edge $\phi=\alpha_2=100^\circ$. The surfaces $\mathfrak{s}_1$ and $\mathfrak{s}_2$ intersect along the rays $(\theta,\phi)=(\pm\theta_0,\phi_0)$, each of which also belongs to one of the surfaces $\mathfrak{s}_\mathrm{r}$ and $\mathfrak{s}_\mathrm{s}$ discussed above.

After the domains $\mathfrak{G}_n$, $n=1,2$, are specified, the components U_n of the decomposition (2.7) are computed by the formulae

$$U_n=\begin{cases}S_n & \text{inside } \mathfrak{G}_n,\\ 0 & \text{outside } \mathfrak{G}_n,\end{cases} \tag{2.20}$$

where S_n is the diffracted component of the solution of an auxiliary problem of diffraction of the plane wave U_0 by the half-plane $\vartheta_n=0$ given in the cylindrical coordinates $(\varrho_n,\vartheta_n,\zeta_n)$ from (2.10), (2.11). Such a field S_n has an explicit analytic representation (Felsen & Marcuvitz 1972),

$$S_n(r,\theta,\phi)=\mathrm{e}^{\mathrm{i}k\zeta_n\zeta_n^0}S(k\varrho_n\varrho_n^0,\vartheta_n;\vartheta_n^0), \tag{2.21}$$

where $(\varrho_n,\vartheta_n,\zeta_n)$ are the cylindrical coordinates (2.9), (2.10) and $S(\varrho,\vartheta;\vartheta_0)$ is the diffracted component of the solution of the classical two-dimensional Sommerfeld problem of diffraction of a plane wave $\mathrm{e}^{\mathrm{i}k\varrho\cos(\vartheta-\vartheta_0)}$ by a half-plane $\vartheta=0$. It is well known (Bowman *et al.* 1969; Felsen & Marcuvitz 1972; Sommerfeld 1898) that $S(\varrho,\vartheta;\vartheta_0)$ is defined by the formulae

$$S(r,\vartheta;\vartheta_0)=(S_+-S_-)\mathrm{e}^{\mathrm{i}kr}, \tag{2.22}$$

where

$$S_\pm=\mathrm{sgn}(\vartheta_\pm)F(2\eta_\pm)\mathrm{e}^{-2\mathrm{i}\eta_\pm^2}, \tag{2.23}$$

$$\eta_\pm=\sqrt{k\varrho}\,|\sin\vartheta_\pm|,\qquad \vartheta_+=\vartheta+\vartheta_0-2\pi,\qquad \vartheta_-=\vartheta-\vartheta_0 \tag{2.24}$$

and

$$F(\eta)=\frac{1}{\sqrt{\pi\mathrm{i}}}\int_\eta^\infty \mathrm{e}^{\mathrm{i}\mu^2}\,\mathrm{d}\mu\equiv\frac{1}{\sqrt{\pi}}\int_{\eta/\sqrt{\mathrm{i}}}^\infty \mathrm{e}^{-s^2}\,\mathrm{d}s \tag{2.25}$$

is the slightly modified Fresnel integral.

Next we compute the secondary conical waves U_1^m and U_2^m, with $m=1,2,\ldots,M$. This can be done by straightforward decomposition of the fields U_1, U_2 on the plane waves followed by application of formulae like (2.21)–(2.25). However, to eliminate technical difficulties, which may conceal the basic ideas of the method, we assume that the configuration of the problem satisfies the conditions

$$(0,\alpha_1)\notin\mathfrak{G}_1,\qquad (0,\alpha_2)\notin\mathfrak{G}_2,$$

which guarantee that the secondary conical waves are not generated.

To conclude this section it is instructive to notice that the waves U_1 and U_2 diffracted by the edges of the screen have discontinuities not only on the surfaces $\mathfrak{s}_1$ and $\mathfrak{s}_2$ involved in (2.20), but also on the surfaces $\mathfrak{s}_\mathrm{r}$ and $\mathfrak{s}_\mathrm{s}$, where the reflected and shadow waves have discontinuities. However, each of the sums $\tilde{U}_1=U_\mathrm{r}+U_\mathrm{s}+U_1$ and $\tilde{U}_2=U_\mathrm{r}+U_\mathrm{s}+U_2$ remain smooth on $\mathfrak{s}_\mathrm{r}$ and $\mathfrak{s}_\mathrm{s}$, although these sums are discontinuous along the corresponding boundaries $\mathfrak{s}_1$ and $\mathfrak{s}_2$.

3. The Liouville representation of the diffracted field

The analysis in the previous section makes it clear that all of the already specified components $U_{\rm s}$, $U_{\rm r}$, U_1 and U_2 of the decomposition (2.7) are piecewise continuous functions satisfying the Helmholtz equation, and that their sum,

$$\tilde{U} = U_{\rm s} + U_{\rm r} + U_1 + U_2, \tag{3.1}$$

satisfies both the Helmholtz equation and the boundary condition from (2.4), but has discontinuities along the surface

$$\mathfrak{s} = \mathfrak{s}_1 \cup \mathfrak{s}_2, \tag{3.2}$$

composed of the circular cones $\mathfrak{s}_1$ and $\mathfrak{s}_2$ described in the previous section and shown in figure 3. This observation leads to the conclusion that the unknown component $U_{\rm d}$ of (2.7) representing waves diffracted by the tip of the screen $\Gamma(\alpha_1, \alpha_2)$ must be a piecewise continuous solution of the Dirichlet problem

$$\nabla^2 U_{\rm d} + k^2 U_{\rm d} = 0, \qquad U_{\rm d}|_{\Gamma} = 0, \tag{3.3}$$

which satisfies the condition at infinity,

$$U_{\rm d}(r, \theta, \phi) = C(\theta, \phi)\frac{{\rm e}^{{\rm i}kr}}{kr}(1 + o(1)), \quad r \to \infty, \tag{3.4}$$

where $C(\theta, \phi)$ is an unspecified function of the angular variables known as the diffraction coefficient, and the interface conditions

$$[U_{\rm d}]_{\mathfrak{s}} = -[\tilde{U}]_{\mathfrak{s}}, \qquad g\left[\frac{\partial U_{\rm d}}{\partial \boldsymbol{n}}g\right]_{\mathfrak{s}} = -g\left[\frac{\partial \tilde{U}}{\partial \boldsymbol{n}}g\right]_{\mathfrak{s}}, \tag{3.5}$$

where the symbol $[\mathcal{F}]_{\mathfrak{s}}$ denotes the jump of the function $\mathcal{F}$ on the surface $\mathfrak{s}$, and $\boldsymbol{n}$ is a unit normal to $\mathfrak{s}$.

To formulate the interface conditions (3.5) in an unambiguous form, we need to designate the orientation of the surface $\mathfrak{s}$. Referring to figure 3, we denote by $\mathfrak{s}_n^+$ the side of the surface $\mathfrak{s}_n$, $n = 1, 2$, facing the interior of the cone $\mathfrak{G}_n$ defined by (2.19) and bounded by $\mathfrak{s}_n$. Similarly, the notation $\mathfrak{s}_n^-$ is reserved for the opposite side of $\mathfrak{s}_n$. Then the junctions $\mathfrak{s}_+ = \mathfrak{s}_1^+ \cup \mathfrak{s}_2^+$ and $\mathfrak{s}_- = \mathfrak{s}_1^- \cup \mathfrak{s}_2^-$ are naturally considered as the inner and outer sides of the surface $\mathfrak{s} = \mathfrak{s}_1 \cup \mathfrak{s}_2$, which makes it possible to define the jump $[\mathcal{F}]_{\mathfrak{s}}$ of the function $\mathcal{F}$ as the difference

$$[\mathcal{F}]_{\mathfrak{s}} = \mathcal{F}|_{\mathfrak{s}_+} - \mathcal{F}|_{\mathfrak{s}_-}. \tag{3.6}$$

After the meaning of the symbol $[\mathcal{F}]_{\mathfrak{s}}$ is specified, we can compute the right-hand sides of the interface conditions (3.5). Taking into account the formulae of the previous section explicitly describing all of the components of the sum $\tilde{U}$ from (3.1), we readily find that

$$[\tilde{U}]_{\mathfrak{s}} = \begin{cases} S_1 & \text{on } \mathfrak{s}_1, \\ S_2 & \text{on } \mathfrak{s}_2, \end{cases} \quad \text{and} \quad \left[\frac{\partial \tilde{U}}{\partial \boldsymbol{n}}\right]_{\mathfrak{s}} = \begin{cases} \partial S_1/\partial \boldsymbol{n} & \text{on } \mathfrak{s}_1, \\ \partial S_2/\partial \boldsymbol{n} & \text{on } \mathfrak{s}_2, \end{cases} \tag{3.7}$$

where S_1 and S_2 are the functions introduced in (2.21). Then, computing these functions by (2.22), we arrive at the expression

$$[\tilde{U}]_{\mathfrak{s}} = F, \qquad F(r, \theta, \phi) = \begin{cases} {\rm e}^{{\rm i}k\zeta_1\zeta_1^0} S(k\varrho_1\varrho_1^0, \vartheta_1; \vartheta_1^0) & \text{on } \mathfrak{s}_1, \\ {\rm e}^{{\rm i}k\zeta_2\zeta_2^0} S(k\varrho_2\varrho_2^0, \vartheta_2; \vartheta_2^0) & \text{on } \mathfrak{s}_2, \end{cases} \tag{3.8}$$

where $(\varrho_n, \vartheta_n, \zeta_n)$, $n = 1, 2$, are the cylindrical coordinates (2.8)–(2.10) of the point (r, θ, ϕ) and the function $S(\varrho, \vartheta; \vartheta_0)$ is defined by (2.22)–(2.25). Then, observing that, on the cones $\mathfrak{s}_n$, the operator of normal differentiation is defined as

$$\frac{\partial}{\partial \boldsymbol{n}} = \vartheta_n^0 \frac{\partial}{\partial \varrho_n} - \varrho_n^0 \frac{\partial}{\partial \vartheta_n} \quad \text{on } \mathfrak{s}_n, \quad n = 1, 2, \tag{3.9}$$

we straightforwardly derive that $\partial S_n / \partial \boldsymbol{n}|_{\mathfrak{s}_n} = 0$, which results, after substitution into (3.7), in the identity

$$g \left[\frac{\partial \tilde{U}}{\partial \boldsymbol{n}} g \right]_{\mathfrak{s}} = 0. \tag{3.10}$$

We seek the solution U_{d} of the problem (3.3)–(3.5), (3.8), (3.10) in the Liouville product form

$$U_{\mathrm{d}}(r, \theta, \phi) = u(r, \theta, \phi) \mathrm{e}^{\mathrm{i}kr}, \tag{3.11}$$

where $u(r, \theta, \phi)$ is a new unknown function.

Substitution of (3.11) into the Helmholtz equation (3.3) and evaluation of the derivatives in spherical coordinates results in the equation

$$\frac{\mathrm{i}}{2k} \left[\frac{\partial^2 u}{\partial r^2} + \frac{2}{r} \frac{\partial u}{\partial r} + \frac{1}{r^2} \left(\frac{\partial^2 u}{\partial \theta^2} - \tan\theta \frac{\partial u}{\partial \theta} \right) + \frac{1}{r^2 \cos^2\theta} \frac{\partial^2 u}{\partial u^2} \right] - \frac{\partial u}{\partial r} - \frac{u}{r} = 0, \tag{3.12}$$

which has to be satisfied by the amplitude $u(r, \theta, \phi)$ from (3.11). Multiplying (3.12) by $q = -\mathrm{i}kr^2$ and rearranging the order of the terms, we arrive at the equation

$$\left[\tfrac{1}{2} r^2 \frac{\partial^2 u}{\partial r^2} + r(1 + \mathrm{i}kr) \frac{\partial u}{\partial r} \right] + \left[\frac{1}{2} \frac{\partial^2 u}{\partial \theta^2} - \tfrac{1}{2} \tan\theta \frac{\partial u}{\partial \theta} \right] + \frac{1}{2\cos^2\theta} \frac{\partial^2 u}{\partial \phi^2} + \mathrm{i}kru = 0, \tag{3.13}$$

which has to be solved subject to the boundary conditions

$$u(r, 0, \phi) = 0 \quad \text{for } \alpha_1 < \phi < \alpha_2 \tag{3.14}$$

and the condition at infinity,

$$u(r, \theta, \phi) = O(1/r), \quad r \to \infty, \tag{3.15}$$

following, respectively, from (3.3), (3.11) and (3.4). Additionally, $u(r, \theta, \phi)$ has to obey the interface conditions

$$u|_{\mathfrak{s}_+} - u|_{\mathfrak{s}_-} = f, \qquad \left. \frac{\partial u}{\partial \boldsymbol{n}} \right|_{\mathfrak{s}_+} - \left. \frac{\partial u}{\partial \boldsymbol{n}} \right|_{\mathfrak{s}_-} = 0, \tag{3.16}$$

with the right-hand side

$$f(r, \theta, \phi) = -\mathrm{e}^{-\mathrm{i}kr} F(r, \theta, \phi) \tag{3.17}$$

involving the function $F(r, \theta, \phi)$ from (3.8).

The principal justification for the conversion of the original problem of diffraction by a plane sectorial screen to the problem (3.13)–(3.16) is that an exact and explicit solution of the latter problem can be obtained in a simple probabilistic form that is convenient both for qualitative analysis and numerical simulation. Such a solution will be derived in § 5 after a brief discussion of the employed probabilistic technique in § 4.

4. Probabilistic solutions of partial differential equations

It is well known (Dynkin 1965; Freidlin 1985) that the classical Dirichlet problem

$$\sum_{n=1}^{N}\left(\tfrac{1}{2}\sigma_n^2\frac{\partial^2 u}{\partial x_n^2}+A_n\frac{\partial u}{\partial x_n}\right)+Bu=0,\qquad u|_{\partial}G=f, \tag{4.1}$$

with real-valued coefficients σ_n and A_n, has the explicit solution

$$u(x)=\boldsymbol{E}\left\{f(\boldsymbol{\xi}_\tau)\exp\left(\int_0^\tau B(\boldsymbol{\xi}_s)\,\mathrm{d}s\right)\right\}, \tag{4.2}$$

where $\boldsymbol{E}$ denotes the average computed over trajectories of the random motion

$$\boldsymbol{\xi}_t=(\xi_t^1,\xi_t^2,\dots,\xi_t^N) \tag{4.3}$$

running across the N-dimensional domain G in accordance with the rules described below. The motion starts at $t=0$ from the point $\boldsymbol{\xi}_0=\boldsymbol{x}$, and it stops at the exit time τ defined as the first instant when $\boldsymbol{\xi}_t$ touches the boundary ∂G. In the time-interval from $t=0$ to $t=\tau$, the motion is controlled by Ito's stochastic differential equations,

$$\mathrm{d}\xi_t^n=\sigma_n(\boldsymbol{\xi}_t)\,\mathrm{d}w_t^n+A_n(\boldsymbol{\xi}_t)\,\mathrm{d}t,\quad \xi_0^n=x_n,\quad n=1,2,\dots,N, \tag{4.4}$$

where the w_t^n are independent one-dimensional Brownian motions. The representation (4.2)–(4.4) is widely known as the Feynman–Kac solution, and in Simon (1979) one may find references to numerous proofs of these formulae based on different ideas and applying different hypotheses on the regularity of the functions σ_n, A_n, B and f, as well as of the boundary ∂G from (4.1).

For practical purposes, the continuous random motion $\boldsymbol{\xi}_t$ governed by (4.3), (4.4) can be approximated by the discrete random walk

$$\boldsymbol{x}\equiv\boldsymbol{\xi}_0\to\boldsymbol{\xi}_1\to\cdots\to\boldsymbol{\xi}_\nu\to\boldsymbol{\xi}_{\nu+1}\to\cdots, \tag{4.5}$$

consisting of instant jumps following each other with the time increment $\Delta t=\varepsilon^2\ll 1$ and determined by the rule

$$\boldsymbol{\xi}_\nu\to\boldsymbol{\xi}_{\nu+1}=\boldsymbol{\xi}_\nu+\varepsilon\breve{S}(\boldsymbol{\xi}_\nu)\cdot\boldsymbol{w}_\nu+\varepsilon^2\boldsymbol{A}(\boldsymbol{\xi}_\nu), \tag{4.6}$$

where

$$\breve{S}=\mathrm{diag}[\sigma_1,\sigma_2,\dots,\sigma_N]\quad\text{and}\quad\boldsymbol{A}=(A_1,A_2,\dots,A_N) \tag{4.7}$$

are the diagonal matrix and the vector formed by the coefficients of the equation (4.1), and

$$\boldsymbol{w}_\nu=(\underbrace{\pm1,\pm1,\dots,\pm1}_{N\text{ components}}) \tag{4.8}$$

is a random vector that may take one of $2N$ different equally probable values.

The Feynman–Kac formula (4.2) solving the fundamental Dirichlet problem (4.1) can be used for derivation of probabilistic solutions of many modifications of (4.1), including an important problem for this work consisting of the homogeneous equation and the boundary conditions,

$$\sum_{n=1}^{N}\left(\tfrac{1}{2}\sigma_n^2\frac{\partial^2 u}{\partial x_n^2}+A_n\frac{\partial u}{\partial x_n}\right)+Bu=0,\qquad u|_{\partial}G=0, \tag{4.9}$$

accompanied by the non-homogenous interface conditions

$$u|_{\mathfrak{s}_+} - u|_{\mathfrak{s}_-} = f, \qquad \left.\frac{\partial u}{\partial \boldsymbol{n}}\right|_{\mathfrak{s}_+} - \left.\frac{\partial u}{\partial \boldsymbol{n}}\right|_{\mathfrak{s}_-} = 0, \tag{4.10}$$

where $\mathfrak{s}_\pm$ are the different sides of the surface $\mathfrak{s} \subset G$ and $\boldsymbol{n} = \boldsymbol{n}(x)$ is the unit normal to $\mathfrak{s}$ oriented towards the side $\mathfrak{s}_+$. Thus it is shown below that the solution of the problem (4.9), (4.10) is delivered by the mathematical expectation

$$u(x) = \boldsymbol{E}\left\{ \sum_{\tau_\nu < \tau} \delta_\nu f(\boldsymbol{\xi}_{\tau_\nu}) \exp\left(\int_0^{\tau_\nu} B(\boldsymbol{\xi}_{\mathrm{s}})\, \mathrm{d}s \right) \right\}, \tag{4.11}$$

computed over the trajectories of the random motion $\boldsymbol{\xi}_t$, which starts at $t = 0$ from the point $\boldsymbol{\xi}_0 = \boldsymbol{x}$ and stops at the exit time τ when it reaches ∂G. In the interval from $t = 0$ to $t = \tau$, the motion $\boldsymbol{\xi}_t$ is controlled by the stochastic equations (4.4), and it touches the interface $\mathfrak{s}$ at the discrete times $t = \tau_\nu$ enumerated by the integer ν, which also parametrizes the factor δ_ν defined by the rule

$$\delta_\nu = \begin{cases} 1 & \text{if } \boldsymbol{\xi}_{\tau_\nu - 0} \in \mathfrak{s}_+ \text{ and } \boldsymbol{\xi}_{\tau_\nu + 0} \in \mathfrak{s}_-, \\ -1 & \text{if } \boldsymbol{\xi}_{\tau_\nu - 0} \in \mathfrak{s}_- \text{ and } \boldsymbol{\xi}_{\tau_\nu + 0} \in \mathfrak{s}_+, \\ 0 & \text{if } \boldsymbol{\xi}_{\tau_\nu - 0} \in \mathfrak{s}_\pm \text{ and } \boldsymbol{\xi}_{\tau_\nu + 0} \in \mathfrak{s}_\pm, \end{cases} \tag{4.12}$$

assigning the value $\delta_\nu = \pm 1$ if, at time $t = \tau_\nu$, the interface $\mathfrak{s}$ is crossed from the side $\mathfrak{s}_\pm$ to the side $\mathfrak{s}_\mp$, but assigning the value $\delta_\nu = 0$ if the surface $\mathfrak{s}$ is not crossed.

To derive formula (4.11), we use the notation $\boldsymbol{\xi}_\pm$ for the point $\boldsymbol{\xi} \in \mathfrak{s}$ considered to be located on the side $\mathfrak{s}_\pm$ of the surface $\mathfrak{s}$. Then the interface conditions (4.10) can be written as

$$\left.\begin{aligned} u(\boldsymbol{\xi}_+) - u(\boldsymbol{\xi}_-) &= f(\boldsymbol{\xi}), \\ [u(\boldsymbol{\xi} + \varepsilon\boldsymbol{n}) - u(\boldsymbol{\xi}_+)] + [u(\boldsymbol{\xi} - \varepsilon\boldsymbol{n}) - u(\boldsymbol{\xi}_-)] &= o(\varepsilon), \end{aligned}\right\} \tag{4.13}$$

which results in either of two equivalent formulae,

$$\left.\begin{aligned} u(\boldsymbol{\xi}_+) &= \boldsymbol{E}\{u(\boldsymbol{\xi} + \varepsilon\boldsymbol{n}), u(\boldsymbol{\xi} - \varepsilon\boldsymbol{n}) + f(\boldsymbol{\xi})\}, \\ u(\boldsymbol{\xi}_-) &= \boldsymbol{E}\{u(\boldsymbol{\xi} - \varepsilon\boldsymbol{n}), u(\boldsymbol{\xi} + \varepsilon\boldsymbol{n}) - f(\boldsymbol{\xi})\}, \end{aligned}\right\} \tag{4.14}$$

where $\boldsymbol{E}\{a_1, a_2\}$ denotes the arithmetic mean of two equally possible values a_1 and a_2.

For any point $\boldsymbol{x} \in G$, we compute $u(x)$ by the Feynman–Kac formula (4.2) applied to the smallest sub-domain of G containing $\boldsymbol{x}$ and bounded by pieces of the interface $\mathfrak{s}$ and of the external boundary ∂G. This generates the representation

$$u(x) = \boldsymbol{E}\left\{ \chi_\tau(\tau_1) u(\boldsymbol{\xi}_{\tau_1}) \exp\left(\int_0^{\tau_1} B(\boldsymbol{\xi}_{\mathrm{s}})\, \mathrm{d}s \right) \right\}, \quad \boldsymbol{\xi}_{\tau_1} \in \mathfrak{s}, \tag{4.15}$$

where τ is the exit time when $\boldsymbol{\xi}_t$ touches the screen, τ_1 is the crossing time defined as the first time when $\boldsymbol{\xi}_t$ reaches the interface $\mathfrak{s}$ and

$$\chi_\tau(t) = \begin{cases} 1 & \text{if } t \geqslant \tau, \\ 0 & \text{if } t < \tau \end{cases} \tag{4.16}$$

is the Heaviside function, which insures that the factor $\chi_\tau(\tau_1)$ vanishes if $\boldsymbol{\xi}_t$ hits the external boundary ∂G before reaching the interface $\mathfrak{s}$. Obviously, $\boldsymbol{\xi}_{\tau_1}$ reaches $\mathfrak{s}$ from the side which is closer to the initial point x. For definiteness, we assume that this is the side $\mathfrak{s}_+$, i.e. we assume that $\boldsymbol{\xi}_{\tau_1} \in \mathfrak{s}_+$. Then, applying (4.14), we represent $u(\boldsymbol{\xi}_{\tau_1})$ as

$$u(\boldsymbol{\xi}_{\tau_1}) = \boldsymbol{E}\{u(\boldsymbol{\xi}_{\tau_1} - \varepsilon\boldsymbol{n}), u(\boldsymbol{\xi}_{\tau_1} - \varepsilon\boldsymbol{n}) + f(\boldsymbol{\xi}_{\tau_1})\} + o(\varepsilon), \quad \boldsymbol{\xi}_{\tau_1} \in \mathfrak{s}_+, \tag{4.17}$$

and, after straightforward substitution of (4.17) into (4.15), we arrive at the representation

$$u(x) = \boldsymbol{E}\left\{\chi_\tau(\tau_1)[\delta_1 f(\boldsymbol{\xi}_{\tau_1}) + u(\boldsymbol{\xi}_{\tau_1} \pm \varepsilon\boldsymbol{n})] \exp\left(\int_0^{\tau_1} B(\boldsymbol{\xi}_s)\,\mathrm{d}s\right)\right\} + o(\varepsilon), \tag{4.18}$$

with the value of δ_1 assigned by (4.12), and with the averaging over the trajectories of the random motions $\boldsymbol{\xi}_t$ on the time-interval $t \in [0, \tau_1)$, and over the random selection of the sign in $u(\boldsymbol{\xi}_{\tau_1} \pm \varepsilon\boldsymbol{n})$. Since the points $\boldsymbol{\xi}_{\tau_1} \pm \varepsilon\boldsymbol{n}$ are located outside the interface $\mathfrak{s}$, the values $u(x_1)$ appearing in the right-hand side of (4.18) can be again computed by (4.18), and continuing further the recursions we eventually arrive, after passing to the limit $\varepsilon \to 0$, at the representation (4.11) of the solution of the problem (4.9), (4.10).

5. Probabilistic representation of the diffracted field

Application of the probabilistic technique to the problem (3.13)–(3.16) is based on the observation that equation (3.13) matches the structure (4.1) with the variables x_n introduced as

$$x_1 = r, \qquad x_2 = \theta, \qquad x_3 = \phi, \tag{5.1}$$

and with the coefficients σ_n, A_n, B defined in the variables x_n by the formulae

$$\sigma_1 = x_1^2, \qquad \sigma_2 = 1, \qquad \sigma_3 = \frac{1}{\cos^2(x_2)}, \tag{5.2}$$

$$A_1 = x_1(1 + \mathrm{i}kx_1), \qquad A_2 = -\tfrac{1}{2}\tan(x_2), \qquad A_3 = 0, \qquad B = \mathrm{i}kx_1. \tag{5.3}$$

The results of the previous section suggest that the solution of the equation (3.13) with the coefficients from (5.2) and (5.3) is closely connected with the trajectories of the three-component random motion $\boldsymbol{\xi}_t = (\xi_t^1, \xi_t^2, \xi_t^3)$ governed by the stochastic differential equations

$$\mathrm{d}\xi_t^1 = \xi_t^1\,\mathrm{d}w_t^1 + \xi_t^1(1 + \mathrm{i}k\xi_t^1)\,\mathrm{d}t, \qquad \xi_0^1 = r, \tag{5.4}$$

$$\mathrm{d}\xi_t^2 = \mathrm{d}w_t^2 - \tfrac{1}{2}\tan(\xi_t^2)\,\mathrm{d}t, \qquad \xi_0^2 = \theta, \tag{5.5}$$

$$\mathrm{d}\xi_t^3 = \mathrm{d}w_t^3/\cos(\xi_t^2), \qquad \xi_0^3 = \phi, \tag{5.6}$$

driven by the independent one-dimensional Brownian motions w_t^1, w_t^2 and w_t^3. These three stochastic motions split into two groups independent of each other: the 'radial' scalar motion ξ_t^1 and the two-dimensional 'angular' motion described by the pair (ξ_t^2, ξ_t^3). From (5.5) and (5.6), we see that the angular motion (ξ_t^2, ξ_t^3) remains real-valued at any time and that it may be considered as a Brownian motion on the two-dimensional unit sphere $\mathbb{S}^2$ parametrized by the angles $(x_2, x_3) \equiv (\theta, \phi)$. On the

contrary, equation (5.4) has a complex drift coefficient $A_1 = x_1(1 + \mathrm{i}kx_1)$, which forces ξ_t^1 to leave the real axis and run across the complex plane. In Budaev & Bogy (2003*a*), the structure of random motions of the type ξ_t^1 is discussed in more detail and, in particular, it is shown that ξ_t^1 is always located in the half-plane $\operatorname{Re}\xi_t^1 \geqslant 0$ and that the drift drags ξ_t^1 towards the point $\xi_* = \mathrm{i}/k$, so that, as $t \to \infty$, the motion ξ_t^1 becomes a random walk in the vicinity of ξ_*.

From the above, it follows that the three-dimensional random process $\boldsymbol{\xi}_t = (\xi_t^1, \xi_t^2, \xi_t^3)$ defined by stochastic equations (5.4), (5.5) may be regarded as a random motion in the four-dimensional space $\mathbb{C} \times \mathbb{S}^2$, where $\mathbb{S}^2 \subset \mathbb{R}^3$ is the two-dimensional unit sphere. The fact that $\boldsymbol{\xi}_t$ leaves the real space makes it impossible to compute the amplitude $u(r, \theta, \phi)$ of the diffracted field by straightforward application of the probabilistic formula (4.11) to the problem (3.13)–(3.16) with the boundary and interface conditions imposed on a two-dimensional surface $\mathfrak{s} \subset \mathbb{R}^3$, which, in general, has zero probability to be hit by one-dimensional trajectories of $\boldsymbol{\xi}_t$ running in the four-dimensional domain $\mathbb{C} \times \mathbb{S}^2$. Nevertheless, there is an indirect way to apply the probabilistic formula (4.11) to the problem (3.13)–(3.16).

Let $\mathfrak{s}_0 \subset \mathbb{S}^2$ be a line on the unit sphere $\mathbb{S}^2$ defined in the angular coordinates (θ, ϕ) as

$$\mathfrak{s}_0 : \theta = 0, \quad \alpha_1 < \phi < \alpha_2. \tag{5.7}$$

Then the cone G from (2.5) can be considered as the direct product

$$G = \mathbb{R}_+ \times (\mathbb{S}^2 \setminus \mathfrak{s}_0) \tag{5.8}$$

of the real semi-axis $\mathbb{R}_+$ corresponding to the radial coordinate $r > 0$ and of the piece $\mathbb{S}^2 \setminus \mathfrak{s}_0$ of the unit sphere $\mathbb{S}^2$ corresponding to the angular coordinates (θ, ϕ). This cone G is naturally imbedded in the four-dimensional domain

$$G^{\mathrm{c}} = \mathbb{C} \times (\mathbb{S}^2 \setminus \mathfrak{s}_0), \tag{5.9}$$

obtained from G by allowing the radial coordinate to have arbitrary complex values.

Next we notice that all of the coefficients of the equation (3.13) and the function $f(r, \theta, \phi)$ from the right-hand sides of the interface conditions (3.16) are analytic with respect to the variable r. This observation makes it possible to consider the problem (3.13)–(3.16) in the four-dimensional complex domain G^{c} from (5.9) with the boundary and interface conditions imposed on the three-dimensional manifolds described in spherical coordinates (r, θ, ϕ) by the conditions $r \in \mathbb{C}$, $(\theta, \phi) \in \mathfrak{s}_n$, $n = 0, 1, 2$, where $\mathfrak{s}_0$ is a line from (5.7) and $\mathfrak{s}_1$, $\mathfrak{s}_2$ are the lines from (3.16). Then, applying formula (4.11), we readily conclude that, for any pair of real angles (θ, ϕ) and for any complex radius r, the solution $u(r, \theta, \phi)$ of the problem (3.13)–(3.16) can be represented by the mathematical expectation

$$u(r, \theta, \phi) = \boldsymbol{E}\left\{ \sum_{\tau_\nu < \tau} \delta_\nu f(\boldsymbol{\xi}_{\tau_\nu}) \exp\left(\int_0^{\tau_\nu} \mathrm{i}k\xi_t^1 \, \mathrm{d}t \right) \right\}, \qquad \boldsymbol{\xi}_0 = (r, \theta, \phi), \tag{5.10}$$

where $f(x)$ is the function from (3.17) defined on the interface $\mathfrak{s}$. The averaging is computed over the trajectories of the stochastic motion $\boldsymbol{\xi}_t = (\xi_t^1, \xi_t^2, \xi_t^3)$, which starts at $t = 0$ and runs thereafter across G^{c}, touching the interface $\mathfrak{s}$ at the discrete crossing times $t = \tau_\nu$.

It is remarkable that the integral in the exponent of (5.10) admits explicit representation

$$\int_0^t \mathrm{i}k\xi_t^1\,\mathrm{d}t = \ln(\xi_t^1) - \ln(\xi_0^1) - w_t^1 - \tfrac{1}{2}t, \tag{5.11}$$

where w_t^1 is the one-dimensional Brownian motion involved in the definition (5.4) of the motion ξ_t^1. Indeed, equation (5.4) yields

$$\mathrm{i}k\xi_t^1\,\mathrm{d}t = \frac{\mathrm{d}\xi_t^1}{\xi_t^1} - \mathrm{d}w_t^1 - \mathrm{d}t, \tag{5.12}$$

and Ito's formula of stochastic differentiation (Dynkin 1965; Feller 1967) generates the identity

$$\mathrm{d}\ln(\xi_t^1) = \frac{\mathrm{d}\xi_t^1}{\xi_t^1} - \frac{1}{2}\left(\frac{\mathrm{d}\xi_t^1}{\xi_t^1}\right)^2 \equiv \frac{\mathrm{d}\xi_t^1}{\xi_t^1} - \tfrac{1}{2}\mathrm{d}t, \tag{5.13}$$

which, when combined with (5.12), leads to the expression

$$\mathrm{i}k\xi_t^1\,\mathrm{d}t = \mathrm{d}\ln(\xi_t^1) - \mathrm{d}w_t^1 - \tfrac{1}{2}\mathrm{d}t, \tag{5.14}$$

equivalent to (5.11).

Finally, taking into account the initial condition $\xi_0^1 = r$, we substitute (5.11) into (5.10) and then (5.10) into (3.11). As a result, we arrive at the formula

$$U_{\mathrm{d}}(r,\theta,\phi) = \frac{\mathrm{e}^{\mathrm{i}kr}}{r}\boldsymbol{E}\left\{\sum_{\tau_\nu<\tau}\delta_\nu\xi_{\tau_\nu}^1 f(\boldsymbol{\xi}_{\tau_\nu})\exp(-w_{\tau_\nu}^1 - \tfrac{1}{2}\tau_\nu)\right\}, \qquad \boldsymbol{\xi}_0 = (r,\theta,\phi), \tag{5.15}$$

which represents the diffracted field $U_{\mathrm{d}}(r,\theta,\phi)$ in a form that emphasizes its structure at infinity, $r\to\infty$, suggested by the radiation condition (3.4).

In conclusion, it is instructive to discuss some of the advantageous features of the probabilistic solution (5.15) of the problem of diffraction (3.3)–(3.5). First, we observe that the convergence of the sum in (5.15) is guaranteed by the well-known (Dynkin 1965; Feller 1967) asymptote $\boldsymbol{E}(|w_t^1|) = O(\sqrt{t})$ as $t\to\infty$, which bounds the average deviation of the Brownian motion w_t^1 in the limit $t\to\infty$. Due to this estimate, the exponent in (5.15) decays as $O(\mathrm{e}^{-q\nu})$ with $q>0$. As for the factors $f(\boldsymbol{\xi}_{\tau_\nu})$ and $\xi_{\tau_\nu}^1$, they remain finite because $f(\boldsymbol{\xi})$ is bounded everywhere due to its definition (3.8), (3.17), and because the drift term of the stochastic equations (5.4) controlling ξ_t^1 drags this motion towards the finite focal point $\xi = \mathrm{i}/k$.

Another attractive feature of the solution (5.15) is that it provides a simple qualitative description of the diffracted field. For instance, the structure of (5.15) makes it clear that, in general, the diffracted field $U_{\mathrm{d}}(r,\theta,\phi)$ decays as $O(1/r)$ as $r\to\infty$. However, if the observation point (r,θ,ϕ) is located close to at least one of the cones $\mathfrak{s}_1$ or $\mathfrak{s}_2$, where $U_{\mathrm{d}}(r,\theta,\phi)$ is discontinuous, then the random motion $\boldsymbol{\xi}_t$ crosses the surface $\mathfrak{s} = \mathfrak{s}_1\cup\mathfrak{s}_2$ soon after it is launched from the point $\boldsymbol{\xi}_0 = (r,\theta,\phi)$, so that, for the ratios $\xi_{\tau_\nu}^1/r$ with small indices, ν takes finite values close to unity. As a result, the field (5.15) does not decay as $r\to\infty$ along the conical surface $\mathfrak{s}$ and the total field (2.7) remains smooth everywhere.

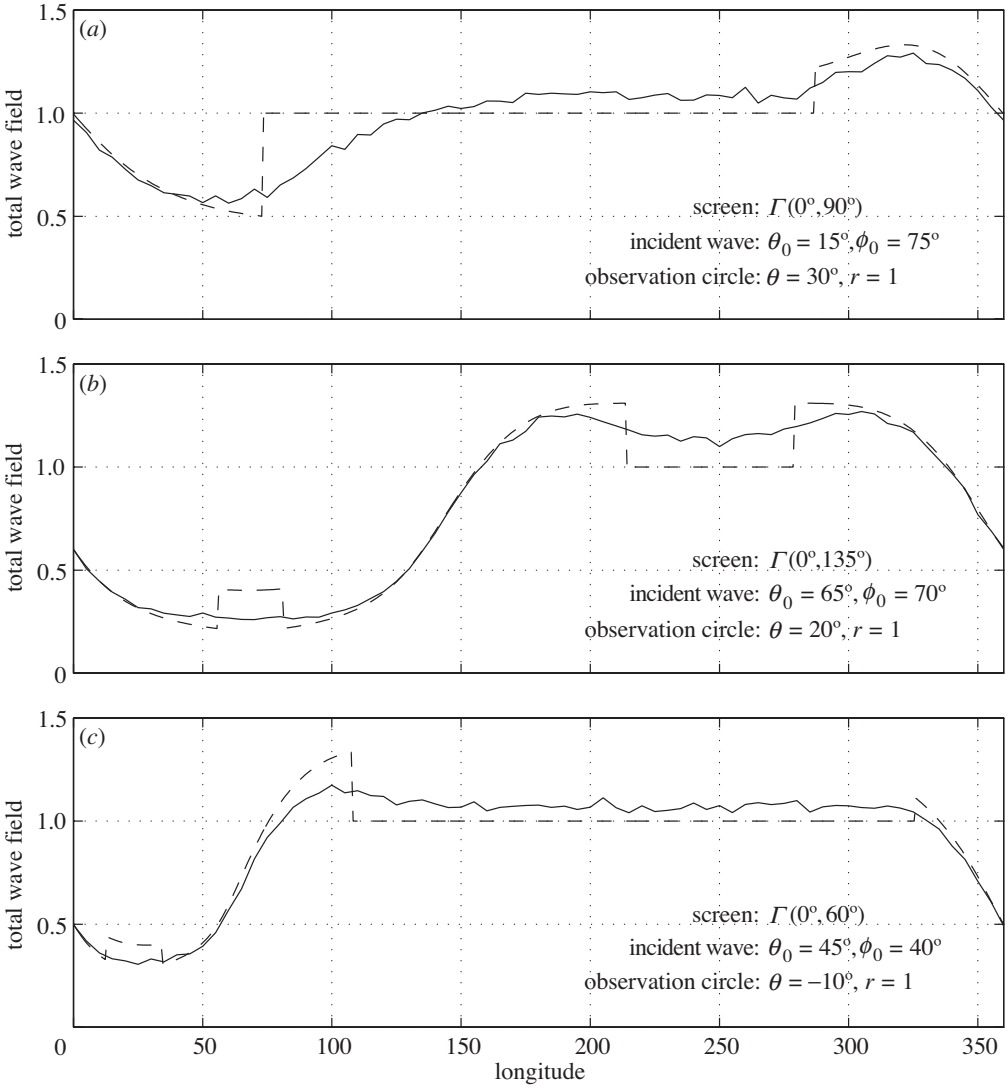

Figure 4. Results of numerical simulation ($N = 10\,000$, $\varepsilon = 0.1$).

6. Numerical examples

To provide an indication of the computational feasibility of the solution (5.15), we used it for numerical simulation of the solutions of some particular problems of diffraction. The results of these simulations are presented in figure 4, consisting of three diagrams corresponding to three different screens.

Part (*a*) of figure 4 presents the amplitude of the total wave field generated due to the diffraction by the quarter plane $\Gamma(0°, 90°)$ of the plane wave propagating in the direction $(\theta_0, \phi_0) = (15°, 75°)$. The results are computed along the horizontal circle $r = 1$, $\theta = 30°$. The dashed line shows the amplitude of the discontinuous field $\tilde{U}$ defined as the superposition (3.1) of the waves described by known analytical

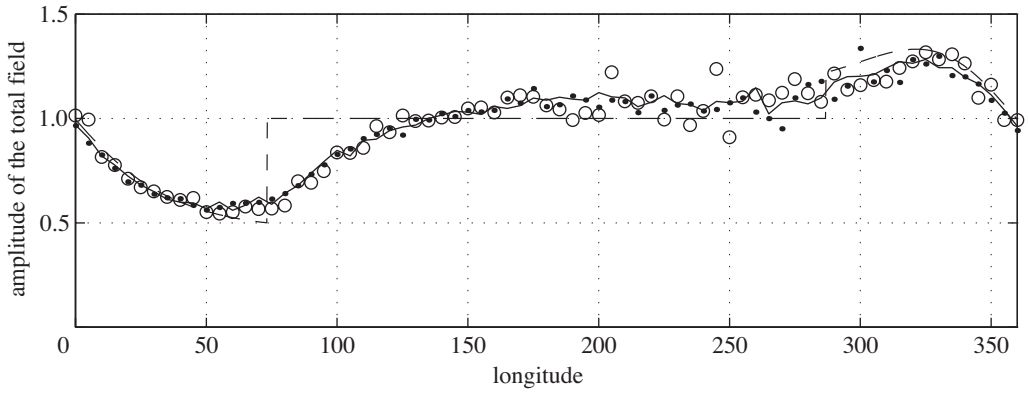

Figure 5. Dependence on the number of averaging random walks.

expressions. The continuous line shows results obtained by adding U_{d} computed by numerical simulation of the mathematical expectation (5.15).

Part (*b*) presents the solution of the problem of diffraction by the screen $\Gamma(0°, 135°)$ of the plane wave propagating in the direction $(\theta_0, \phi_0) = (65°, 70°)$. The results are computed along the circle $r = 1$, $\theta = 30°$ and are shown in the same format as used on the top diagram.

Finally, part (*c*) of figure 4 presents the solution along the circle $r = 1$, $\theta = -10°$ of the problem of diffraction by the screen $\Gamma(0°, 60°)$ of the plane wave propagating in the direction $(\theta_0, \phi_0) = (30°, 20°)$.

All of the simulations were computed by a simple algorithm based on an approximation of the continuous random motion $\boldsymbol{\xi}_t$ satisfying stochastic equations (5.4)–(5.6) by discrete random walks of the type (4.5)–(4.8), with the fixed spatial step $\varepsilon = 0.1$. The crossing points $\boldsymbol{\xi}_{\tau_\nu}$ where the motion $\boldsymbol{\xi}_t$ intersects the cones $\mathfrak{s}_1$ and $\mathfrak{s}_2$ were approximated by the nodes of the discrete random walk located outside of the corresponding cone. The Fresnel integrals (2.25) were approximated by a Taylor power series, and the mathematical expectation in (5.15) was approximated by the averaging of $N = 10\,000$ random walks. The algorithm was implemented in a simple MATLAB code, and although no special effort was made for its optimization, we were able to carry out all computations on a Notebook PC with a 900 Mhz processor.

Theoretically, the accuracy of the numerical scheme increases to zero error when the adjustable parameters ε and N tend to the limits $\varepsilon \to 0$ and $N \to \infty$ in the order suggested by the expression

$$U = \lim_{N\to\infty} \Big(\lim_{\varepsilon\to 0} U^{N,\varepsilon} \Big), \tag{6.1}$$

where U is the exact solution while $U^{N,\varepsilon}$ are the approximations obtained by the averaging of N discrete random walks with the spatial step ε. In practice, this means that for every value of $\varepsilon > 0$, the accuracy of the approximation $U^{N,\varepsilon}$ increases as N grows until some threshold N_ε, after which a further increase of N makes no sense without decreasing ε.

The convergence of the approximations $U^{N,\varepsilon}$ as $N \to \infty$ is illustrated in figure 5, which is similar to the top diagram of figure 4 in all aspects except that figure 5 shows the solutions obtained by the averaging of 500 (open circles), 1000 (dots) and 4000 (solid line) random walks with $\varepsilon = 0.1$, while figure 4 shows the result of averaging

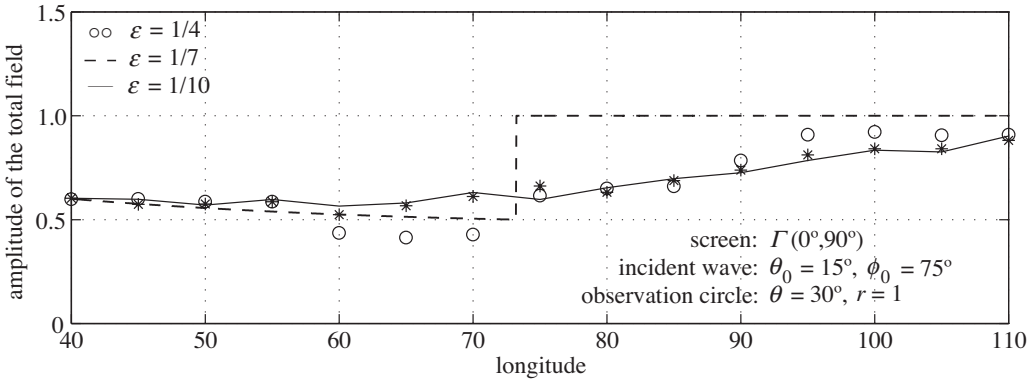

Figure 6. Dependence on the step of the random walk ($N = 10\,000$).

10 000 random walks. These graphs also demonstrate that the number of random walks required for obtaining stable numerical results depends on the location of the points where the wave field is computed. Thus, in the domain with the longitudes $\phi \approx \frac{1}{2}(\alpha_1 + \alpha_2) = 45°$, the convergence is better and the averaging of 500 random walks with the $\varepsilon = 0.1$ step provides the same accuracy as the averaging of 4000 or more random walks with the same spatial step. However, in the area most difficult for convergence with longitudes $\phi \approx \pi + \frac{1}{2}(\alpha_1 + \alpha_2) = 225°$, the results stabilize after the averaging of at least 4000 random walks. In general, numerical experiments agree with the rate of convergence typical for probabilistic methods which require the averaging of four times as many random walks to achieve two times better accuracy.

The dependence of the approximations $U^{N,\varepsilon}$ on the step ε of the discrete random walks is illustrated in figure 6, which plots the solutions for different ε of the same problem considered in figure 5 and in the first diagram of figure 4. The graphs of figure 6, obtained by the averaging of 10 000 random walks with the steps $\varepsilon = \frac{1}{4}$, $\varepsilon = \frac{1}{7}$ and $\varepsilon = \frac{1}{10}$, demonstrate that, near the surface, where the geometric field $\tilde{U}$ from (2.7) has discontinuities (jumps in the dashed line), the decrease in ε improves the quality of the approximation. However, in the domain remote from the discontinuities of $\tilde{U}$, all of the approximations are very close to each other, although the approximations with larger ε run faster. More precisely, computations with a spatial step of half the size take about four times as long.

Finally, it should be mentioned that the numerical results presented were generated by algorithms which by no means may be considered as optimal and whose sole purpose was to demonstrate the principal feasibility of the probabilistic approach to the problem of diffraction. However, we believe that such obvious improvements as the use of random walks with the step depending on the current position and the use of a better method of computation of the Fresnel integrals can turn our algorithms into a very practical working tool for the simulation of diffraction by wedge-shaped screens.

7. Conclusion

The version of the random-walk method developed in Budaev & Bogy (2003*a*) and employed here results in a simple exact solution of the canonical problem of diffraction of a plane incident wave by a plane wedge-shaped perfectly reflecting screen.

Although the analysis of the present paper is restricted to the cases with no multiple diffraction by the edges of the screen, these restrictions may be straightforwardly lifted by the inclusion in the decomposition (2.7) of additional pre-defined components determined by closed-form analytical expressions.

In this paper we focused on the diffraction problem with the Dirichlet boundary conditions and this restriction resulted in the probabilistic Feynman–Kac formulae (5.10) and (5.15) with the averaging over trajectories of the random motion stopped at the boundary of the domain where the values of the unknown function are pre-assigned by the boundary conditions. However, it is well known (Freidlin 1985) that such formulae can be easily modified to represent solutions of problems with more general impedance boundary conditions of the type (2.6). The only serious modification needed is the extension of the averaging to trajectories which 'bounce' from the boundary according to a specific rule determined by the boundary conditions. We do not discuss this matter in detail in the present paper, which is devoted to the main idea of the method, but we plan to address this more general case in a future paper.

As with analytic or asymptotic methods, probabilistic solutions provided by the random-walk method are local in the sense that they make it possible to compute functions of interest at individual points without computing them on dense meshes. Moreover, such solutions admit simple perfectly scalable implementations with practically unlimited capability for parallel processing, and these solutions admit meaningful physical interpretations which do not contradict, but compliment, elementary models of wave propagation employed by ray theory. All of these features together make the random-walk method attractive, both for qualitative and numerical analysis of the important problem of diffraction by a plane wedge-shaped screen.

This research was supported by NSF Grant CMS-0098418 and by the William S. Floyd Jr Distinguished Professorship in Engineering held by D.B.

References

Bowman, J. J., Senior, T. B. A. & Uslenghi, P. L. E. (eds) 1969 *Electromagnetic and acoustic scattering by simple shapes*. New York: Hemisphere Publishing Corporation.

Budaev, B. V. & Bogy, D. B. 2001 Probabilistic solutions of the Helmholtz equations. *J. Acoust. Soc. Am.* **109**, 2260–2262.

Budaev, B. V. & Bogy, D. B. 2002*a* Analysis of one-dimensional wave scattering by the random walk method. *J. Acoust. Soc. Am.* **111**, 2555–2560.

Budaev, B. V. & Bogy, D. B. 2002*b* Application of random walk methods to wave propagation. *Q. J. Mech. Appl. Math.* **55**, 209–226.

Budaev, B. V. & Bogy, D. B. 2003*a* Random walk approach to wave propagation in wedges and cones. *J. Acoust. Soc. Am.* **114**, 1733–1741.

Budaev, B. V. & Bogy, D. B. 2003*b* Random walk approach to wave radiation in cylindrical and spherical domains. *Prob. Engng Mech.* **18**, 339–348.

Budaev, B. V. & Bogy, D. B. 2004*a* Diffraction by a wedge with different impedance boundary conditions on its faces. (Submitted.)

Budaev, B. V. & Bogy, D. B. 2004*b* Diffraction of a plane wave by a sector with Dirichlet or Neumann boundary conditions. *IEEE Trans. Antennas Propagat.* (In the press.)

Budaev, B. V. & Bogy, D. B. 2004*c* Wave scattering by surface-breaking cracks and cavities. *Wave Motion.* **40**, 163–172.

Dynkin, E. B. 1965 *Markov processes*. Die Grundlehren der Mathematischen Wissenschaften in Einzeldarstellungen, vol. 121–122. Academic.

Feller, W. 1967 *An introduction to probability theory and its applications*. Probability and Mathematical Statistics. Wiley.

Felsen, L. B. & Marcuvitz, N. 1972 *Radiation and scattering of waves*. Microwaves and Fields Series. Englewood Cliffs, NJ: Prentice-Hall.

Fock, V. A. 1965 *Electromagnetic diffraction and propagation problems*. International Series of Monographs on Electromagnetic Waves, vol. 1. Oxford: Pergamon.

Fock, V. A. & Leontovich, M. A. 1946 Solution of the problems of propagation of electromagnetic waves along the Earth's surface by the method of parabolic equation. *J. Phys. USSR* **10**, 1–13.

Freidlin, M. 1985 *Functional integration and partial differential equations*. The Annals of Mathematics Studies, vol. 109. Princeton University Press.

Simon, B. 1979 *Functional integration and quantum physics*. Pure and Applied Mathematics, vol. 86. Academic.

Sommerfeld, A. 1898 Mathematische theorier der diffraction. *Math. Annln* **47**, 317–374.